Excited states of the vacancy in diamond

J. E. Lowther
Department of Physics, University of Witwatersrand, Johannesburg, South Africa
(Received 24 May 1993)

The Coulson-Kearsley molecular model has been applied to various forms of the vacancy in diamond with considerable success from the point of view of group theory. Electron-electron interaction and configuration mixing are two important features of the molecular model which is reexamined with the intention of explaining why the model has been so successful to date. Parameters representing both one-electron and electron-electron interactions are deduced within an empirical framework of the molecular approach and are shown to consistently explain several properties of both GR1 (neutral vacancy) and ND1 (negative vacancy) optical features. Conclusions are reached concerning the position of neutral and negative vacancy energy levels relative to the valence-band edges. It is shown that optical properties of the neutral vacancy and the negative vacancy are strongly affected by charge-transfer excitations such that optical transitions are more probable at V^- than at V^0. The optical transition proababilities for ND1 relate strongly to GR2–8 such that the probability of bound excitonic transitions at V^0 can become considerably enhanced. The molecular multiplet structure of V^0 is extended to include the effects of electron-electron correlation with bound excitonic states and this is shown to explain several properties of GR2–8.

I. INTRODUCTION

Optical properties of diamond are specifically dependent upon the defect character of the material. Of the most common defects, nitrogen holds the important place of being the defect that is now associated with characterizing different types of diamond.[1] Depending upon the nature of nitrogen in the lattice, the diamond is classified as being type IA or IB. Type-IIA diamond also contains nitrogen defects albeit at a much lower level than either of the other types and type-IIB diamond, being very nearly nitrogen free, is found to contain boron. Within the varieties of type-I diamond, differences in character of the nitrogen essentially relate to a spatial separation of the nitrogen atoms (for example, platelets) or to the concentration of carbon vacancies. As far as the electronic properties of such diamonds are concerned, it is vacancies that mainly affect the character of the defects, a variety of different centers having now been identified and attributed to specific vacancy-nitrogen complexes.[2–5]

From the spectroscopic point of view, vacancy-related complexes in diamond always give rise to sharp lines with related phonon sidebands, the latter revealing distinctive dynamic Jahn-Teller character.[6–11] Yet despite a wealth of experimental investigation using both optical[12–22] and magnetic approaches[24–26] the fundamental origin of electronic states associated with the simplest defect in diamond—namely the lattice vacancy—remains essentially an unsolved problem.

The earliest attempt to understand the electronic structure of the diamond vacancy was undertaken within the Hartree-Fock approach by Coulson and Kearsley.[27] Such a model associated the observed electronic transitions with molecular-type excitations among four electrons trapped on equivalent dangling bonds about a vacant lattice site. The defect so described is termed the neutral vacancy V^0 and when five electrons are trapped at the vacant lattice site the negative vacancy V^- is formed. A group theoretical structure of the Coulson-Kearsley model has provided a very successful qualitative framework in which several optical features found in irradiated diamond have now been understood, so that now the so-called GR1 band (which has a zero-phonon line at 1.673 eV) is definitely associated with V^0 and the ND1 feature (with zero-phonon line at 3.149 eV) with V^-. Magnetic resonance work on both of these centers[24,25] is totally consistent with the Coulson and Kearsley model[28] providing further confirmation of the identity of these defects.

On the other hand, despite the good group theoretic understanding, theory at the *ab initio* level has failed to give a quantitative account of the properties of these defects, despite several different attempts at enumerating the various molecular integrals encountered in the Coulson and Kearsley model.[29–33] Likewise one-electron calculations[34–38] using a variety of *ab initio* approaches while having a common degree of group theoretic similarity in that the symmetry of vacancy-related levels is always predicted to be that same (a_1 or t_2 in the tetrahedral point group T_d), have differed considerably in the conclusions made over the importance of electron-electron correlation which is the main feature of the Coulson-Kearsley model. Notwithstanding such computational differences, it cannot be disputed that the essential predictions of the Coulson-Kearsley model agree with experimental observation and therefore present overwhelming support that electron-electron correlation is indeed an important interaction at both V^0 and V^-.

Also associated with the carbon vacancy are lines lying between 2.881 and 3.007 eV in the optical spectrum and which have been labeled GR2–8. Unlike GR1 and ND1 the nature of these lines is not yet established despite considerable experimental investigation[39,40] as well as

theoretical debate.[41–44] Spectroscopy has indicated that GR2–8 are related to both GR1 and ND1; for example, piezospectroscopy has revealed that GR2–8 has the same ground state as GR1 (E symmetry in the tetrahedral point group T_d) (Ref. 39) and other measurements have revealed a direct correlation of the GR1 and GR2–8 optical intensities.[40] Photoconductivity has also indicated that electrical carriers (holes) are produced under GR2–8 excitation,[45,46] whereas no conduction is associated with GR1 even though the photoconduction spectra show distinct reductions of current. As with GR2–8, free carriers are associated with ND1 excitation[47] and again there is similarity in that neither center gives rise to any luminescence.[18] A collective interrelation between GR1, GR2–8, and ND1 is also observed under photoexcitation at energies less than 3.150 eV. Here the intensity of the ND1 optical spectra can be increased, whereas with excitation above 3.15 eV GR1 is enhanced.[48]

It is clear that from these observations GR1, GR2–8, and the ND1 system are all closely related and with the assignment of GR1 to V^0 and ND1 to V^-, GR2–8 must somehow be associated with a reaction $V^- \rightarrow V^0 + e^-$.

In this paper we shall review molecular modeling of the neutral vacancy in diamond. First we shall accept that previous calculations of the molecular model have not been successful and rather we shall propose that an empirical approach be adopted. We shall see that this will yield significant insight into the relative locations of the neutral and negative vacancy levels and at the same time offer us a clue as to the origin of GR2–8. Then we shall examine the actual mechanism of optical transitions at both neutral and negative vacancies and how these can affect transitions related to GR2–8. Finally we look at the modification of the vacancy energy levels because of electron-electron interaction with localized excitonic states.

II. MOLECULAR MODELS OF VACANCIES IN DIAMOND

The point symmetry of the diamond lattice is T_d and about a vacant lattice site four sp^3 carbon hybrids give rise to one-electron states with a_1 and t_2 symmetry. Relative to each of the sp^3 hybrids shown in Fig. 1, these one-electron states have the specific form

$$\begin{aligned} a_1 &= \tfrac{1}{2}[\varphi_1+\varphi_2+\varphi_3+\varphi_4] , \\ t_2x &= \tfrac{1}{2}[\varphi_1+\varphi_2-\varphi_3-\varphi_4] , \\ t_2y &= \tfrac{1}{2}[\varphi_1-\varphi_2-\varphi_3+\varphi_4] , \\ t_2z &= \tfrac{1}{2}[\varphi_1-\varphi_2+\varphi_3-\varphi_4] . \end{aligned} \tag{1}$$

In diamond, electron-electron correlation leads to a multiplet structure with ${}^1E(a_1^2t_2^2)$ and ${}^4A_2(a_1^2t_2^3)$ being the lowest energy states observed for V^0 and V^-, respectively. Transitions to the states ${}^1T_2(a_1^2t_2^2)$ and ${}^4T_1(a_1t_2^4)$ are then associated with GR1 and ND1. Energies of the molecular multiplets have been expressed within the Hartree-Fock approximation through a series of one and two center integrals which were denoted as being A-B and C-K, respectively, in the early work of Coulson and Kearsley. Table I contains some numerical values of these integrals as evaluated by several authors. Although there are subtle levels of approximation in each of these calculations, as has been pointed out recently,[12] such a molecular approach at calculating the multiplet structure has, in general, met with very little success.

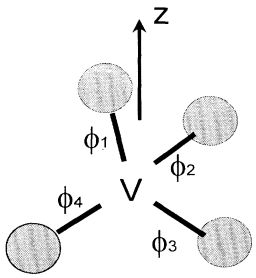

FIG. 1. Molecular bonds about the lattice vacancy.

On the other hand, far more sophisticated electronic-structure calculations have been restricted to evaluating the one-electron nature of the vacancy levels and their location relative to the bulk-band edges. Of particular significance has been the separation in energy between the one-electron a_1 and t_2 states as measured by a splitting parameter Δ, some calculated values of which are shown in Table II. The local-density values are taken as quoted[38] although the a_1 levels probably extend over a significant region into the valence band. A common feature to have emerged from these calculations is that a_1 lies only slightly below the valence-band edge, E_V, whereas t_2 lies above E_V.

A. Empirical model for GR1 and ND1

The two-center many-electron integrals appearing in Table I can be grouped into two types, direct or Coulomb (J) and exchange integrals (K), the difference between the two types of integrals coming from the statistical nature of the electron distribution such that

$$J = \int \psi_a(r_1)\psi_b(r_2)\frac{1}{r_{12}}\psi_c(r_1)\psi_d(r_2)\mathbf{dr} = [\psi_a\psi_b\psi_c\psi_d] \tag{2}$$

and

$$K = \int \psi_a(r_1)\psi_b(r_2)\frac{1}{r_{12}}\psi_c(r_2)\psi_d(r_1)\mathbf{dr} = [\psi_a\psi_b\psi_d\psi_c] . \tag{3}$$

TABLE I. Molecular integrals: Δ one-electron splitting; C–F are Coulomb and G–K are exchange. All are expressed in eV.

Refs.	Δ	C	D	E	F	G	J	K
Ref. 27	6.70	10.9	11.3	10.9	11.1	2.85	2.83	2.76
Ref. 31	8.42	10.5	11.1	10.7	11.0	3.04	3.21	3.06
Ref. 29	10.16	9.8	8.7	9.4	8.3	1.79	0.68	1.23
Ref. 33	8.68	5.7	2.8	3.6	2.3	0.83	0.47	0.0

TABLE II. Calculated one-electron energy levels of the neutral vacancy relative to the valence bands. All values are in eV.

Approach	a_1	t_2	Δ
Huckel, Ref. 34	$E_V-0.4$	$E_V+1.0$	1.4
Huckel, Ref. 35	$E_V-1.4$	$E_V+1.2$	2.6
CNDO, Ref. 36	$E_V-0.1$	$E_V+2.0$	2.1
Local density, Ref. 38	$E_V-2.0$	$E_V+1.5$	3.5

The early work of Coulson-Kearsley related such integrals with similar atomic quantities—as discussed this approach has met with little quantitative success. However, this does not necessarily mean that the basis of the Coulson-Kearsley formalism is incorrect because fundamentally the model is group theoretical in concept. One notable feature of the model is that it includes configuration mixing which in the case of GR1 allows for the interaction between multiplets arising from the one-electron configurations $a_1^2t_2^2$, $a_1t_2^3$, and t_2^4. A simple empirical approximation of the Coulson-Kearsley model would be to measure this interaction by taking *all* the Coulomb integrals and *all* the exchange integrals to be equal. The multiplet energies in the system can then be expressed using the molecular model in terms of parameters Δ_{V^0}, J, and K, with the role of configuration interaction essentially being measured through the parameter K. In the case of V^0 the multiplets have energies which are given from the following interaction matrices:

$$
\begin{aligned}
{}^1E &: \begin{bmatrix} X & \sqrt{6}K & K \\ \sqrt{6}K & X+\Delta_{V^0} & -\sqrt{6}K \\ K & -\sqrt{6}K & X+2\Delta_{V^0} \end{bmatrix}, \\
{}^1T_2 &: \begin{bmatrix} X & \sqrt{2}K & K \\ \sqrt{2}K & S+\Delta_{V^0} & -\sqrt{2}K \\ K & -\sqrt{2}K & X+2\Delta_{V^0} \end{bmatrix}, \\
{}^3T_1 &: \begin{bmatrix} X-3K & -\sqrt{2}K & K \\ -\sqrt{2}K & X+\Delta_{V^0} & \sqrt{2}K \\ K & \sqrt{2}K & X+2\Delta_{V^0} \end{bmatrix}, \\
{}^1A_1 &: \begin{bmatrix} X & 2K \\ 2K & X+2\Delta_{V^0} \end{bmatrix},
\end{aligned}
\tag{4, 5}
$$

and

$$
\begin{aligned}
&{}^1T_1: {}^3E:{}^3A_2:{}^3T_2:X+\Delta_{V^0}-2K , \\
&{}^5A_2: X+\Delta_{V^0}-6K ,
\end{aligned}
\tag{6}
$$

where

$$X=4\langle t_2\rangle+6J \tag{7}$$

is such that $\langle t_2\rangle$ is the one-electron energy of the t_2 molecular orbital. In Fig. 2 we show energies of these states expressed in units of Δ_{V^0} as the ratio K/Δ_{V^0} varies, and we also indicate transitions associated with the GR1 center, and those which we shall relate with GR2–8.

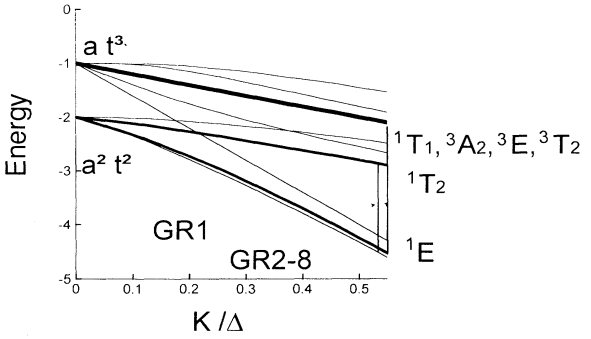

FIG. 2. Multiplets of the neutral vacancy V^0. Energy is expressed in units of Δ.

Similarly as shown in Fig. 3 we can express energies of the multiplet states of the negative vacancy in terms of the integrals J and K and a one-electron energy difference Δ_{V^-} as follows:

$$
{}^2E : \begin{bmatrix} Y & \sqrt{6}K \\ \sqrt{6}K & Y+\Delta_{V^-} \end{bmatrix}, \quad {}^2T_1 : \begin{bmatrix} Y & \sqrt{3}K \\ \sqrt{3}K & Y+\Delta_{V^-} \end{bmatrix}, \tag{8}
$$

$$
{}^2T_2 : \begin{bmatrix} Y & -K & \sqrt{2}K \\ -K & Y+\Delta_{V^-} & \sqrt{2}K \\ \sqrt{2}K & \sqrt{2}K & Y+2\Delta_{V^-} \end{bmatrix}, \tag{9}
$$

and

$$
{}^2A_1 : Y-2K+\Delta_{V^-} : {}^4A_2 : Y-6K : {}^4T_1 : Y-6K+\Delta_{V^-} , \tag{10}
$$

where

$$Y=5\langle t_2\rangle+10J . \tag{11}$$

We have knowingly taken the J and K integrals to be the same for V^0 and V^-, but because of differences in occupancy of the vacancy t_2 orbital it is highly unlikely that Δ_{V^0} and Δ_{V^-} are the same. The empirical model for the multiplet structure of *both* V^0 and V^- is therefore

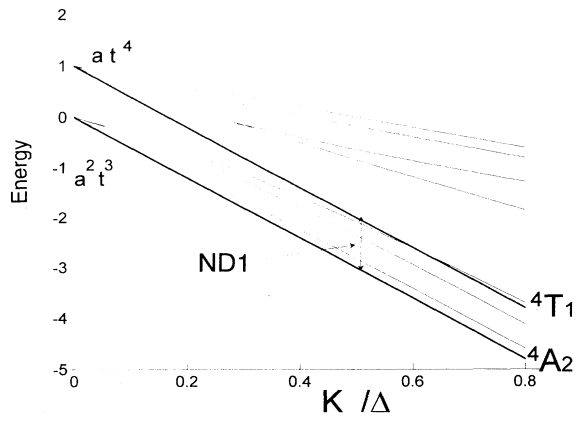

FIG. 3. Multiplets of the negatively charged vacancy V^-. Energy is expressed in units of Δ.

now expressed solely in terms of the parameters Δ_{V^0}, Δ_{V^-}, and K.

B. One-electron and multiplet levels relative to valence band

To estimate the parameters J and K we here make the proposal (which shall be borne out later in the paper) that the excited state of GR2–8 relates to the $^1T_1$ multiplet in the $a_1 t_3^3$ configuration of V^0, and then we require that

$$\frac{E(^1T_1)-E(^1E)}{E(^1T_1)-E(^1E)}=\frac{E(\mathrm{GR1})}{E(\mathrm{GR2})}=\frac{1.673}{2.881}=0.58\ . \quad (12)$$

From Eqs. (4) and (6) we deduce for the neutral vacancy that $K=0.58$ eV and $\Delta_{V^0}=1.39$ eV, which is very near the values tabulated in Table II. In the case of V^-, Eq. (10) readily leads to $\Delta_{V^-}=3.15$ eV. To continue further we make use of the established result that holes are produced under optical excitation of the ND1 center and take the ground state of V^- at or in the valence band. As the ND1 lines are sharp it seems reasonable to take $E(^4A_2)\simeq E_V$, and so measuring energies from the valence-band edge ($E_V=0$) a relationship between the one-electron energy $\langle t_2\rangle$ and parameters J and K can thereafter be deduced using Eqs. (11) and (10) to be

$$\langle t_2\rangle=\frac{6K-10J}{5}\ . \quad (13)$$

Clearly we have that $J<\frac{6}{10}K$ for the t_2 level to be above the valence band, and in Fig. 4 we show the energy of the multiplet levels of the neutral vacancy relative to those of V^-. In particular, we note that at $J\simeq 0$, the ground multiplet of V^0 is also near the valence-band edge. Similarly we can obtain the location of the one-electron energies $\langle a_1\rangle$ and $\langle t_2\rangle$ and which are similarly shown in Fig. 5. Taking $J=0$ we are therefore able to derive the relative location of both one-electron and multiplet levels relative to the valence band as indicated in Fig. 6. We see in the case of V^0 that the a_1 level is located very near the valence-band edge—again consistent with many of the electronic-structure calculations [especially using complete neglect of differential overlap (CNDO)] as inspection of Table II readily reveals.

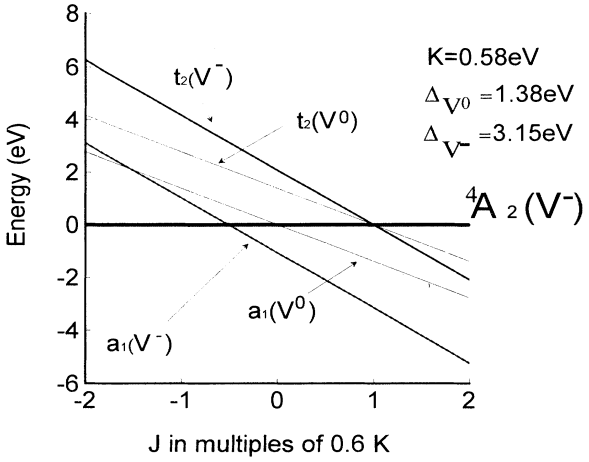

FIG. 5. Relative energy of one-electron vacancy levels.

C. Validity of simple Hartree models for GR1 and ND1

Group theoretically the lowest configuration $a_1^2 t_2^2$ has often been found to be more than adequate when analyzing perturbations on the GR1 and ND1 line spectra. Therefore to measure the amount of $a_1^2 t_2^2$ character in the ground state of GR1 we shall employ the empirical model discussed earlier. For example, writing the ^1E state as

$$|^1E\rangle=\alpha|^1E(a_1^2t_2^2)\rangle+\beta|^1E(a_1t_2^3)\rangle+\gamma|^1E(t_2^4)\rangle \quad (14)$$

then the eigenvector α which measures the extent of $a_1^2 t_2^2$ can be obtained from Eq. (4) for various values of the ratio K/Δ. Similarly writing the $^1T_2$ level as

$$|^1T_2\rangle=\alpha'|^1T_2(a_1^2t_2^2)\rangle+\beta'|^1T_2(a_1t_2^3)\rangle+\gamma'|^1T_2(t_2^4)\rangle \quad (15)$$

and again obtaining α' from the appropriate matrix in Eq. (4) the contribution of the lowest one-electron contri-

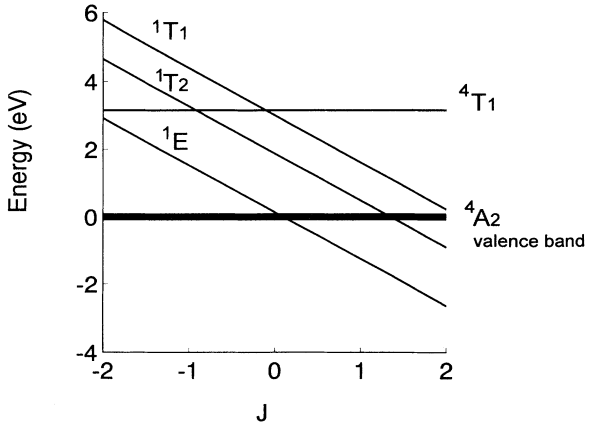

FIG. 4. Relative energy multiplets of GR1 and ND1.

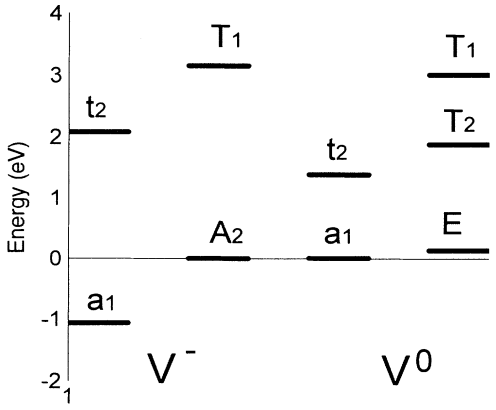

FIG. 6. One-electron and multiplet levels of the negative and neutral vacancy relative to the valence-band edge ($E=0$).

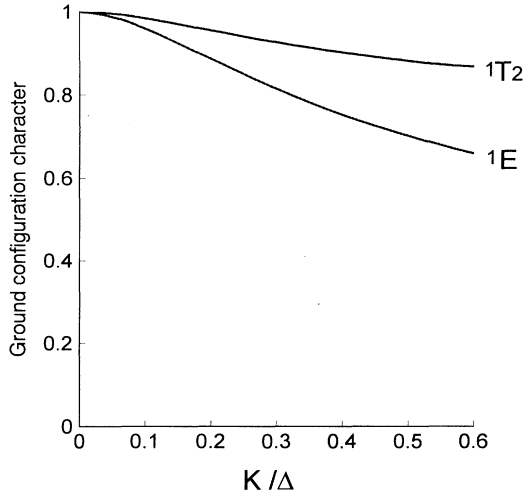

FIG. 7. $a_1^2t_2^2$ character in the two multiplet states of the GR1 line.

bution can be gauged. Both α and α' are displayed in Fig. (7). Clearly we see that with the value of K/Δ_{V^0} deduced above that both ^1E and $^1T_2$ are composed mainly of $a_1^2t_2^2$ character.

III. OPTICAL TRANSITIONS AT GR1 AND ND1

Optical spectroscopy has without doubt played a very important role in the characterization of vacancy-related defects in diamond. The vibronic structure has been studied both experimentally and theoretically such that the Jahn-Teller nature of the defect is now reasonably well understood.[6] However, a point that has been alluded to is the underlying mechanism of how the transition takes place in the first place. Optical transitions in solids are primarily of two types: either atomic where the transition is associated with a single atom or else of a charge-transfer nature where interatomic processes are involved. In the case of vacancy-related structures both types of mechanisms are possible. Group theory shows that electric dipole transitions at both V^0 and V^- can be accounted for in terms of only two matrix elements as follows: for ND1

$$\langle {}^4A_2|\mathbf{r}|{}^4T_1z\rangle=\langle a_1|\mathbf{r}|t_2\zeta\rangle \ ; \tag{16}$$

for GR1

$$\langle {}^1E\theta|\mathbf{r}|{}^1T_2\zeta\rangle=\frac{2}{\sqrt{3}}\langle t_2\xi|\mathbf{r}|t_2\eta\rangle \ . \tag{17}$$

To evaluate such matrix elements we make use of standard molecular-orbital techniques which show that each can be specified in terms of three distinct contributions. For example, along the z direction indicated in Fig. 1, the electric dipole vector has the following contributions at each of the four carbon atoms about the vacancy:

$$z\mathbf{k}=(z_i+d)\mathbf{k}$$

$$\text{with } d=+a \ (i=1,2) \text{ and } d=-a \ (i=3,4) \ , \tag{18}$$

where $2a$ is the cube side length in which the tetrahedron can be inscribed. Then the *atomic* contribution to the matrix elements involves

$$\langle\phi_i|z\mathbf{k}|\phi_i\rangle=[a\pm\langle s|z|p_z\rangle]$$

$$(+ \text{ for } i=1,2 \text{ and } - \text{ for } i=3,4) \ . \tag{19}$$

If we use a simple Slater description of the atomic orbitals s and p_z in the form

$$|s\rangle=\left[\frac{\alpha^5}{3\pi}\right]^{1/2}re^{-\alpha r} \text{ and } |p_z\rangle=\left[\frac{\alpha^5}{\pi}\right]^{1/2}ze^{-\alpha r} \tag{20}$$

we obtain for the *atomic* contribution,

$$\langle s|z|p_z\rangle=\frac{5}{2\sqrt{3}\alpha} \ . \tag{21}$$

A *charge-transfer* contribution to the electric dipole-matrix element again involves the s and p orbitals but now with interaction between adjacent ϕ bonds. Each of these can be resolved into σ and π components depending upon the relative orientation of the bond-orbital states. Such components (now evaluated at a distance of $\sqrt{8}a$ when there is no lattice relaxation) are defined as follows:

$$A_{\sigma,\pi}=\langle s_i|z_j|p_{z,j}\rangle \text{ and } B_{\sigma,\pi}=\langle s_i|z_i|p_{z,j}\rangle \ , \tag{22}$$

for example, in the case of the ϕ_1 and ϕ_2 bond orbitals there are only π contributions to the dipole-matrix element along the z direction whereas for ϕ_1 with ϕ_3 and ϕ_4 both σ and π terms are involved. Finally there is a third contribution to the dipole-matrix element which comes about because of overlap on the adjacent bond orbitals. As with the charge-transfer terms this can be resolved into σ and π diatomic overlap integrals S_s, $S_{p\sigma}$, and $S_{p\pi}$. Eventually we find that the matrix elements evaluated along the z direction take the form, for ND1

$$\langle a_2|\mathbf{r}|t_2\zeta\rangle=0.5(a-\langle s|z|p_z\rangle)-A_\sigma-A_\pi+B_\sigma$$

$$-B_\pi+0.25a(3S_s-S_{p\sigma}-S_{p\pi}) \ ; \tag{23}$$

for GR1,

$$\langle t_2\xi|\mathbf{r}|t_2\eta\rangle=0.5(a-\langle s|z|p_z\rangle)$$

$$+A_\pi-B_\pi-0.25a(S_s+S_{p\pi}) \ . \tag{24}$$

It is particularly instructive to consider the magnitude of the separate contributions to each of the matrix elements, and these are given in Table III. From Eqs. (16) and (17) we therefore deduce that the overall intensity of the ND1

TABLE III. Relative contributions to the ND1 and GR1 electric dipole-matrix elements (using Slater orbital with exponent 1.625 a.u. approximate to atomic carbon).

Contribution	$\langle a_1\|r\|t_2\zeta\rangle$	$\langle t_2\xi\|r\|t_2\eta\rangle$
Atomic	0.3962	0.3962
Charge transfer	0.1797	−0.1032
Overlap	0.0405	−0.0424
Total	0.6165	0.2506

band is intrinsically larger than the intensity of the GR1 band—which would be consistent with some early[49] and more recent[16] observations.

IV. VACANCY-RELATED TRANSITIONS: GR2–8

The mystery of the origin of the GR2–8 lines has remained for some years even though the general consensus of opinion is that the lines relate either directly or indirectly to the interconversion of V^0 to V^-. Piezospectroscopy has now indicated[39] that *all* lines associated with GR2–8 have excited states with T_1 symmetry and this observation has to be accounted for. The principal properties of the GR2–8 series are listed in Table IV.

Various theoretical models have been advanced for the origins of GR2–8 at varying levels of sophistication. A *bound exciton* model was proposed by Dunn[41] in which during the transition $V^0 \rightarrow V^- + e^+$, the hole is strongly bound to V^- during which excitation gives rise to sharp lines. The argument for the nature of the final states is that as V^- has a ground state $^4A_2$ and the hole occupies a state with $^2T_2$ symmetry final coupled states $^3T_1$ and $^5T_1$ result. The model, therefore, required that the ground state of GR2–8 be of symmetry $^3T_1$ to make the transition from V^0 allowed on the basis of spin considerations. Indeed the Coulson-Kearsley model does give the $^3T_1$ multiplet in the V^0 multiplet structure, however, this is not the ground state of GR2–8 which as with GR1 is ^1E. Instead of assuming that the trapped hole be located only in a $^2T_2$ state, Lowther[42] extended the molecular model of the vacancy by suggesting that the localized hole reside in one of the twelve backbonds on the carbon atoms about the vacant atom site. Such backbonds can give rise to one-electron states with symmetries A_1+E+2T_2 about the vacant lattice site and so multiplet states having total spin zero with symmetry T_1 and T_2 result. This model was subsequently criticized by Mainwood[43] on the grounds that semiempirical cluster-model calculations located the one-electron levels associated with the backbond states at some depth into the valence band and it was thus argued that any optical transitions associated with these states would exhibit a broadened structure rather than the sharp features as observed. This argument, however, has overlooked the fact that the GR2–8 transitions are associated with multiplet states rather than solely one-electron levels.

Two other models have also been put forward for the origin of GR2–8. Stoneham[44] has suggested that two-electron transitions are involved. Here one of the two bound t_2 electrons in the ^1E multiplet of GR1 is excited simultaneously with the other electron. The second electron, however, is then excited into a level which in a conventional one-electron excitation is normally forbidden, and thus the final multiplet state of GR2–8 involves a one-electron configuration like t_2x, with x being the symmetry of the additional level. The final model, recently proposed by Prins,[50] is based upon nuclear structure concepts where capture of elementary particles about the nucleus is known to polarize the nucleus and at the same time affect the energy of the state into which the particle is captured. This model therefore differs from the first three in that it involves a dynamic polarization of the electronic charge density at the lattice vacancy.

The importance of electron-electron correlation in regard to the origin of the lines GR2–8 has once again been stressed by Stoneham.[44] Here it was argued that many of the lines have an electronic origin rather than a vibronic nature, a conclusion consistent with that reached from studies of excited states of dynamic Jahn-Teller systems.[51] In this section of the paper we shall now consider the origin of GR2–8 in light of results arising from the empirical model introduced in Sec. II and from investigations of the optical transition probabilities in Sec. III.

TABLE IV. Energies and relative intensities of GR2–8—taken from Ref. 8.

Property	GR2	GR3	GR4	GR5	GR6	GR7	GR8
Energy (eV)	2.881	2.888	2.902	2.940	2.958	2.976	2.997
					2.960	2.982	2.998
							3.002
							3.005
							3.008
Intensity	0.5	1.0	0.02	0.04	0.55	0.13	0.57

A. Electron-electron correlation with bound exciton states

In diamond the spin-orbit interaction is small and unlike many semiconductors a hole in the valence band occupies states with overall nominal T_2 symmetry. Hereafter we label the hole state t_2^* thereby avoiding confusion with the vacancy t_2 state discussed above. In Sec. II we concluded that a neutral vacancy-related a_1 state lay near the valence-band edge, and in Sec. IV pointed out that electronic excitations from such a state involved a substantial degree of interatomic charge transfer making the transition highly probable. The empty a_1 state formed after such transition as occurring in $^1E(a_1^2t_2^2) \rightarrow {}^1T_2(a_1t_2^3)$ would subsequently be filled leaving behind the t_2^* hole. Thus, in a one-electron picture, the transition is from the GR1 ground $a_1^2t_2^2$ configuration excitation to $a_1t_2^3$ or $a_1^2t_2^3t_2^*$. The possible many-electron multiplets that can arise from a $t_2^3t_2^*$ configuration are listed in Table V. Out of these, three $^1T_1$ states are possible and which are derived from $^2E(t_2^3)$, $^2T_1(t_2^3)$, and $^2T_2(t_2^3)$. Now by similar argument $^2E(t_2^3)$ and $^2T_2(t_2^3)$ give rise to the states $^3E(a_1t_2^3)$ and $^3T_2(a_1t_2^3)$, which were the excited states found to be degenerate with $^1T_1(a_1t_2^3)$ according to the model in Sec. II. Thus under *both* $a_1^2t_2^2 \rightarrow a_1t_2^3$ *and* $a_1^2t_2^2 \rightarrow a_1^2t_2^3t_2^*$ excitation, degenerate states with overall T_1 symmetry can result, namely

TABLE V. Allowed multiplets from a $t_2^3t_2^*$ configuration.

t^3	t^3t^*								
$^4A_2$	$^3T_1$	$^5T_1$							
^2E	$^1T_1$	$^3T_1$	$^1T_2$	$^3T_2$					
$^2T_1$	$^1A_2$	$^3A_2$	^1E	^3E	$^1T_1$	$^3T_1$	$^1T_2$	$^3T_2$	
$^2T_2$	$^1A_1$	$^3A_1$	^1E	^3E	$^1T_1$	$^3T_1$	$^1T_2$	$^3T_2$	

$^1T_1(a_1t_2^3)$, $^1T_1a_1^2[^2E(t_2^3)t_2^*]$, and $^1T_1a_1^2[^2T_2(t_2^3)t_2^*]$. Any possible degeneracy of these multiplets will be removed through electron-electron correlation such that the multiplets now have relative energies given from the matrix equation:

$$\begin{bmatrix} \langle a_1\rangle & k_1 & k_2 \\ k_1 & \langle t_2^*\rangle & k_3 \\ k_2 & k_3 & \langle t_2^*\rangle \end{bmatrix}, \tag{25}$$

where $\langle t_2^*\rangle$ is the energy of the bound hole state and

$$k_1=\langle {}^1T_1(a_1t_2^3)\left|\frac{1}{r_{ij}}\right|{}^1T_1a_1^2[^2E(t_2^3)t_2^*]\rangle ,$$

$$k_2=\langle {}^1T_1(a_1t_2^3)\left|\frac{1}{r_{ij}}\right|{}^1T_1a_1^2[^2T_2(t_2^3)t_2^*]\rangle , \tag{26}$$

$$k_3=\langle {}^1T_1a_1^2[^2E(t_2^3)t_2^*]\left|\frac{1}{r_{ij}}\right|{}^1T_1a_1^2[^2T_2(t_2^3)t_2^*]\rangle .$$

Expressing multiplet states in the form of Slater determinants as follows:

$$|{}^1T_1(a_1t_2^3)z\rangle=\frac{1}{\sqrt{2}}(|\overline{a_1}\xi\bar{\xi}\zeta|-|\overline{a_1}\eta\bar{\eta}\zeta|) ,$$

$$|{}^1T_1[^2E(t_2^3)t_2^*]z\rangle=\frac{1}{\sqrt{6}}(2|\xi\eta\zeta\overline{\zeta^*}|-|\xi\bar{\eta}\zeta\overline{\xi^*}|-|\bar{\xi}\eta\zeta\overline{\xi^*}|) , \tag{27}$$

$$|{}^1T_1[^2T_2(t_2^3)t_2^*]z\rangle=-\tfrac{1}{2}(|\xi\zeta\bar{\xi}\overline{\eta^*}|+|\xi\eta\bar{\eta}\overline{\eta^*}| -|\eta\zeta\bar{\zeta}\overline{\xi^*}|-|\xi\bar{\xi}\eta\overline{\xi^*}|) ,$$

where, for example, $\overline{\zeta^*}$ denotes a state with spin $=-\frac{1}{2}$, we find using the notation of Eq. (2) that

$$k_1=-\frac{1}{\sqrt{3}}[\xi\zeta^*\eta a_1] ,$$

$$k_2=\frac{1}{\sqrt{2}}[\xi\zeta^*\eta a_1] , \tag{28}$$

$$k_3=\sqrt{\tfrac{2}{3}}[\xi\zeta^*\zeta\eta^*] .$$

A typical overall $^1T_1$ state is then

$$|{}^1T_1\rangle_i=\alpha_i|{}^1T_1(a_1t_2^3)\rangle+\beta_i|{}^1T_1(^2E(t_2^3)t_2^*)\rangle +\gamma_i|{}^1T_1(^2T_2(t_2^3)t_2^*)\rangle \tag{29}$$

with α_i, β_i and γ_i being given from the matrix in Eq. (25). Expressing each $^1T_1$ state in this way now allows us to evaluate the electric dipole matrix element from the ground ^1E GR1 ground state as

$$\langle {}^1E\theta|\mathbf{r}|{}^1T_1z\rangle=\frac{2}{\sqrt{3}}(\alpha_i\langle a_1|\mathbf{r}|t_2\xi\rangle +\gamma_i\langle t_2^*\eta^*|\mathbf{r}|t_2\xi\rangle) . \tag{30}$$

Now from the results of Sec. III we had

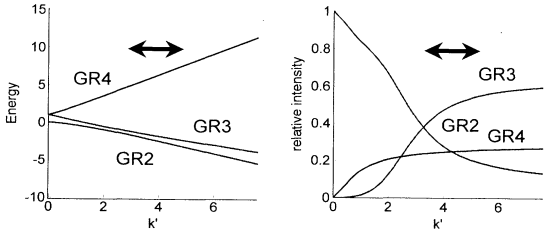

FIG. 8. $^1T_1$ levels and relative intensities of GR2–4 assuming interaction with one exciton state. The arrow indicates the region where there is some agreement with the experimental trend. Energy is expressed in units of $\langle a_1\rangle-\langle t_2^*\rangle$.

$\langle a_1|\mathbf{r}|t_2\zeta\rangle>\langle t_2\xi|\mathbf{r}|t_2\eta\rangle$ and so the intensity of transitions from the ^1E ground state of V^0 to each of the GR2–8 $^1T_1$ excited states will vary approximately according to

$$I(^1E\rightarrow{}^1T_1)\propto\alpha_i^2 . \tag{31}$$

The dependence of relative energies and intensities upon the magnitude of electron-electron correlation as measured by a parameter k or upon the value of the energy difference $\langle a_1\rangle-\langle t_2^*\rangle$ can thus be obtained and this is shown in Fig. 8, where we have used

$$k_1=-\frac{1}{\sqrt{3}}k , \quad k_2=\frac{1}{\sqrt{2}}k , \quad k_3=\sqrt{\tfrac{2}{3}}k \tag{32}$$

as suggested from Eq. (28). The relative splitting in energies follows the trend with those observed for GR2, GR3, and GR4 when the electron-electron correlation is such that $k\sim3$–4 times the $\langle a_1\rangle-\langle t_2^*\rangle$ splitting energy. The analysis of Sec. II suggested that this splitting would be small, thus in turn the value of k is small—probably a few meV.

B. Electron-electron correlation with multiple bound levels

The single-particle energy of a bound state trapped at a defect such as the lattice vacancy can, to a first approximation, be obtained from well-known *standing-wave* solutions of the Schrödinger equation with an infinite potential well. These are given from classical expressions of the form[52]

$$\langle t_2^*\rangle_{l,m,n}=\frac{\hbar^2\pi^2}{2ma^2}(l^2+m^2+n^2)=\delta(l^2+m^2+n^2) \tag{33}$$

with l,m,n being integers and δ some energy parameter. The threefold degenerate levels which we associate with bound exciton states $t_2^*(l,m,n)$ have energies corresponding to $(l,m,n)=(100)$, (110), (200), (210), . . . and of these there are sixfold degeneracies, starting with the $t_2^*(210)$ exciton with energy 5δ. The possible occurrence of multiple bound exciton states was not considered earlier and now the interaction matrix as given by Eq. (25) is extended to become

$$
\begin{array}{cccccccccccc}
\langle a_1 \rangle & k_1 & k_2 & k_1 & k_2 & k_1 & k_2 & k_1 & k_2 & k_1 & k_2 & \cdots \\
k_1 & \delta & k_3 & & & & & & & & & \\
k_2 & k_3 & \delta & & & & & & & & & \\
k_1 & & & 2\delta & k_3 & & & & & & & \\
k_2 & & & k_3 & 2\delta & & & & & & & \\
k_1 & & & & & 4\delta & k_3 & & & & & \\
k_2 & & & & & k_3 & 4\delta & & & & & \\
k_1 & & & & & & & 5\delta & k_3 & k_3^* & k_3 & \\
k_2 & & & & & & & k_3 & 5\delta & k_3 & k_3^* & \\
k_1 & & & & & & & k_3^* & k_3 & 5\delta & k_3 & \\
k_2 & & & & & & & k_3 & k_3^* & k_3 & 5\delta & \\
\vdots & & & & & & & & & & \ddots &
\end{array}
\tag{34}
$$

Diagonalization of this matrix will therefore yield the various excitonic-related $^1T_1$ levels. Employing the values of k_1, k_2, and k_3 as given from Eqs. (28) and (32) the eigenvalues of the above matrix now depend only upon k,δ and a one-electron energy value $\langle a_1 \rangle$. Expressing $\langle a_1 \rangle$ in units of δ the $^1T_1$ multiplet energies can therefore be obtained for various magnitudes of electron correlation interaction as now measured through the parameter k which is also expressed in units of δ. There are several limits of the model corresponding to the location of the a_1 level relative to the t_2^* bound states. We consider specific cases.

1. a_1 vacancy level on a fixed number of bound states

To illustrate the correlated structure for a variable number of bound states we simply use Eq. (34), but for the first bound state the matrix is the upper 3×3 component, with two bound states the matrix is the upper 5×5 component and so on. As indicated in Fig. 9 where we have considered up to four bound states the a_1 level has been positioned at the location of the unperturbed t_2^* bound state. The energy-level structure in the upper left of Fig. 9 is the same as that for Fig. 8, however when there is a configuration interaction with higher exciton states significant modification of the $^1T_1$ energies occurs.

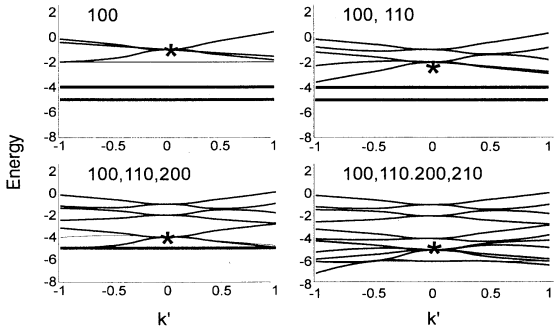

FIG. 9. $^1T_1$ levels for an interaction with a varying number of excitons. The position of the a_1 level relative to exciton energies is denoted by an asterisk. Energy is in units of δ.

This therefore suggests that the relative location of the a_1 level will be an important feature in the energy structure of the correlated system.

2. Fixed location of the a_1 vacancy level (the possible origin of −GR 5–8)

On the other hand, the a_1 level can be fixed in energy *between* a specific number of t_2^* exciton states. To model the situation (which we suggest could be applicable to GR2–8) the matrix of Eq. (34) has been employed in taking five t_2^* states and using $\langle a_1 \rangle = 2.5\delta$. To the left of Fig. 10 is shown the energy-level structure and to the right of this is shown the relative intensity of transitions to these levels which have been calculated using the eigenvector of the $^1T_1(a_1 t_2^3)$ state following the method outlined in the above section. As this may be the case applicable to GR2–8, we have indicated in Fig. 10 lines which are observed with largest intensity.

V. DISCUSSION

There is no doubt as to the importance of the vacancy in diamond when it comes to optical characteristics and defect properties of the material. Accumulating evidence that many sharp features in the optical spectrum relate, in one way or another, to a vacant lattice site is again in-

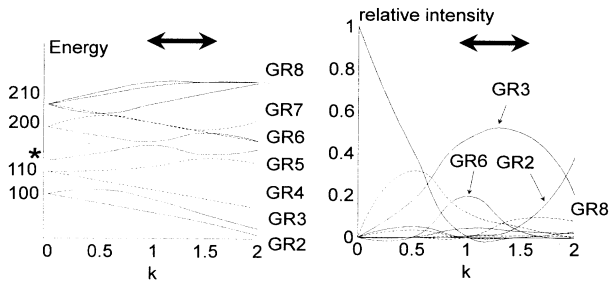

FIG. 10. $^1T_1$ energies (in units of δ) and relative intensities with $\langle a_1 \rangle = 2.5\delta$ (the energy shown by an asterisk) and interacting with four exciton states. The transitions GR2, GR3, GR6, and GR8 are observed to be the most intense.

dicating the importance of this intrinsic defect. In this paper we have attempted to understand essential features of the lattice vacancy exploiting the molecular model put forward some time ago by Coulson and Kearsley, and yet at the same time adopting an empirical approach through which various parameters are deduced from both GR and ND1 optical features. We found in Sec. II that only three parameters Δ_{V^0}, Δ_{V^-}, and K were needed to explain the essential properties of GR1 and ND1 systems. The value $\Delta_{V^0}=1.35$ eV so deduced for the neutral vacancy lies very near that calculated using Huckel theory [1.4 eV (Ref. 34)] or CNDO molecular-orbital parametrization [2.1 eV (Ref. 36)]. We also found that the ground multiplets of both centers are very close to the valence-band edge even though the t_2 one-electron levels from which they are derived lie some way into the gap. At the same time the multiplet structure deduced for the neutral vacancy has suggested a way to interpret the origin of the GR2–8 series of lines.

Configuration interaction which takes place through electron-electron correlation has been an important feature in the model, yet the extent of such mixing is far less than expected from estimates based upon the Coulson-Kearsley model. This therefore explains why the lowest configuration ($a_1^2t_2^2$ for V^0 or $a_1^2t_2^3$ for V^-) has proved very often to be sufficiently adequate when understanding specific properties of both the neutral and negative vacancy.

A feature which hitherto seems to have been overlooked are the relative values of GR1 and ND1 optical transition probabilities as measured through matrix elements like $\langle a_1|\mathbf{r}|t_2\xi\rangle$ and $\langle t_2\xi|\mathbf{r}|t_2\eta\rangle$. Our analysis has indicated that the former matrix element is almost three times larger than the latter because of charge transfer among the four bonds at the vacancy lattice site. This feature, together with the extremely large degeneracy of levels found in an excited state of V^0, has led us to propose a model for the GR2–8 series of lines in which the large value of the matrix element $\langle a_1|\mathbf{r}|t_2\xi\rangle$ and electron-electron interaction between vacancy and bound exciton hole states play important roles. We saw, depending upon the number of bound hole states and the extent of electron-electron correlation, that several closely spaced levels would be possible all with symmetry $^1T_1$. Because each of these contains a contribution from the $^1T_1(a_1t_2^3)$ multiplet of a neutral vacancy and since the $a_1\rightarrow t_2$ optical transition probability is relatively large, wide variations in the observed optical intensities can be observed. This was confirmed from the calculations which in turn are in fair agreement with the observed pattern of GR2, GR3, and GR4 for moderate values of electron-electron correlation. We saw that additional configuration interaction with higher energy hole states through electron-electron correlation would improve agreement with experiment and at the same time the additional exciton configurations could be the origin of the GR5–GR8 transitions. The relative location of the vacancy a_1 level and the exciton levels appears to be a significant feature in the model especially when it comes to relative intensities of the GR2–8 lines. We have pointed out that local-density results did not firmly fix a single a_1 level but rather showed a relatively broad distribution of such states below the valence-band edge. The quantitative discrepancy between the results we have obtained here and from experiment therefore can, in part, be attributed to the nonsingular nature of the a_1 level.

The overall number of bound valence (t_2^*) states and why such states arise can, at this stage, only be speculation. Yet one point forthcoming from group theoretic argument is that for only one bound state GR2, GR3, and GR4 are present together—it seems that GR2–4 do have a firm correlation.[44] The other lines GR5–8 would, according to the analysis discussed here, be indicative of an additional number of bound states and since the degeneracy of the exciton states increases to higher hole energy then it is anticipated that the number of lines observed in the GR5–8 series will also increase. The large degeneracy associated with GR8 seems consistent with this conclusion.

Within the model many properties of the neutral and negative vacancy can now be understood. First the GR1 and ND1 lines are sharp because the transitions originate from multiplet states which reside in the energy gap—even though the ground multiplet states for both V^0 and V^- are only slightly above the valence-band edge. Optical transitions at V^0 differ from V^- in that the latter involve transitions between orbitals of different symmetry. During optical excitation the emptied a_1 orbital is subsequently populated from a t_2^* bound hole which, in turn, is released to become mobile. The mechanism of this process is here unspecified but very likely it would involve a Fano type of resonance as suggested by Stoneham[44] with the $a_1\rightarrow t_2$ transition occurring simultaneously with a $t_2^*\rightarrow a_1$ hole transition among the various correlated multiplet states. Irrespective of the specific mechanism, once the holes are released luminescence can no longer take place simply because the ground state is now populated. This situation, which we suggest is responsible for the photoconductivity and absence of luminescence in GR2–8, will also hold for the ND1 transition at V^-. Thus in this respect GR2–8 and ND1 are similar when it comes to emission processes.

[1]Gordon Davies, *Diamond* (Hilger, Bristol, 1983).
[2]Gordon Davies, Proc. R. Soc. London **336**, 507 (1974).
[3]Gordon Davies, J. Phys. C **7**, 3797 (1974).
[4]Gordon Davies and M. F. Hamer, Proc. R. Soc. London Ser. A **348**, 285 (1976).
[5]J. E. Lowther, J. Phys. Chem. Solids **45**, 127 (1984).
[6]Gordon Davies, Rep. Prog. Phys. **4**, 789 (1971).
[7]J. E. Lowther, J. Phys. C **8**, 3448 (1975).
[8]Gordon Davies and C. Foy, J. Phys. C **13**, 2203 (1980).
[9]A. M. Stoneham, Solid State Commun. **21**, 339 (1977).
[10]M. Lannoo and A. M. Stoneham, J. Phys. Chem. Solids **29**, 1987 (1968).

[11]J. Walker, Rep. Prog. Phys. **42**, 108 (1979).
[12]C. D. Clark and E. W. J. Mitchell, Rad. Eff. **9**, 219 (1971).
[13]C. D. Clark and E. W. J. Mitchell, in *Proceedings of Radiation Effects in Semiconductors,* edited by N. B. Urli and J. W. Corbett, IOP Conf. Proc. No. 31 (Institute of Physics and Physical Society, London, 1977), p. 45.
[14]C. D. Clark and C. A. Norris, J. Phys. C **4**, 2223 (1971).
[15]C. D. Clark and J. Walker, Proc. R. Soc. London **334**, 241 (1973).
[16]Gordon Davies, S. C. Lawson, A. T. Collins, A. M. Mainwood, and S. J. Sharp, Phys. Rev. B **46**, 13 157 (1992).
[17]Gordon Davies, Nature (London) **269**, 498 (1977).
[18]Gordon Davies and E. C. Lightowlers, J. Phys. C **3**, 638 (1969).
[19]A. T. Collins, J. Phys. C **11**, 1 (1978).
[20]Gordon Davies, Proc. R. Soc. London. Ser. A **336**, 507 (1974).
[21]Gordon Davies, J. Phys. C **7**, 3797 (1974).
[22]D. S. Nedzveretskii and V. A. Gaisin, Fiz. Tverd. Tela (Leningrad) **14**, 2946 (1973) [Sov. Phys. Solid State **14**, 2535 (1973)].
[23]Gordon Davies and C. M. Penchina, Proc. R. Soc. London Ser. A **338**, 359 (1974).
[24]I. N. Douglas and W. A. Runciman, J. Phys. C **10**, 2253 (1977).
[25]I. N. Douglas and W. A. Runciman Phys. Chem. Min. **1**, 129 (1977).
[26]J. Isoya, H. Kanda, Y. Uchida, S. C. Lawson, and S. Yamasaki, Phys. Rev. B **45**, 1436 (1992).
[27]C. A. Coulson and M. J. Kearsley, Proc. R. Soc. London Ser. A **241**, 433 (1957).
[28]J. E. Lowther and A. M. Stoneham, J. Phys. C **11**, 2165 (1978).
[29]C. A. Coulson and F. P. Larkins, J. Phys. Chem. Solids **32**, 2245 (1971).
[30]J. Friedel, M. Lannoo, and G. Leman, Phys. Rev. **164**, 1056 (1967).
[31]T. Yamagouchi, J. Phys. Soc. Jpn. **17**, 1359 (1962).
[32]W. E. Hagston, J. Phys. C **3**, 791 (1969).
[33]A. M. Stoneham, Proc. Phys. Soc. **88**, 135 (1966).
[34]R. P. Messmer and G. D. Watkins, Phys. Rev. B **7**, 2568 (1973).
[35]F. P. Larkins, J. Phys. Chem. Solids **23**, 965 (1976).
[36]A. Mainwood, J. Phys. C **11**, 2703 (1978).
[37]R. P. Watkins and G. D. Watkins, Phys. Rev. Lett. **32**, 1244 (1975).
[38]G. B. Bachelet, G. A. Baraff, and M. Schluter, Phys. Rev. B **24**, 4736 (1981).
[39]Colleen Foy and Gordon Davies, J. Phys. C **13**, L25 (1980).
[40]A. T. Collins, J. Phys. C **14**, 289 (1981).
[41]D. Dunn (unpublished).
[42]J. E. Lowther, Philos. Mag. **36**, 483 (1977).
[43]A. M. Mainwood, J. Phys. C **11**, L449 (1978).
[44]A. M. Stoneham, Mat. Sci. Engin. B **11**, 211 (1992).
[45]J. Walker, L. A. Vermeulen, and C. D. Clark, Proc. R. Soc. London **341**, 253 (1974).
[46]L. A. Vermeulen, C. D. Clark, and J. Walker, in *Proceedings of Lattice Defects in Semiconductors,* edited by A. Seeger, IOP Conf. Proc. No. 23 (Institute of Physics and Physical Society, London, 1974), p. 294.
[47]R. G. Farrar and L. A. Vermeulen, J. Phys. C **5**, 2762 (1972).
[48]Gordon Davies, in *Chemistry and Physics of Carbon,* edited by P. W. Philips and P. A. Turner (Dekker, New York, 1981), Vol. 13, p. 1.
[49]C. D. Clark, R. W. Ditchburn, and H. B. Dyer, Proc. R. Soc. London Ser. A **234**, 363 (1956).
[50]J. Prins (unpublished).
[51]J. E. Lowther, S. Afr. J. Phys. **4**, 38 (1981).
[52]R. M. Eisberg, *Fundamentals of Modern Physics* (Wiley, New York, 1961).

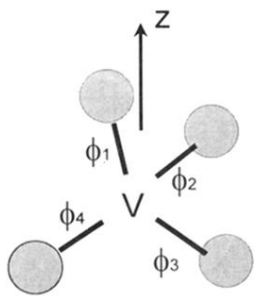

FIG. 1. Molecular bonds about the lattice vacancy.